NASA TM X-652

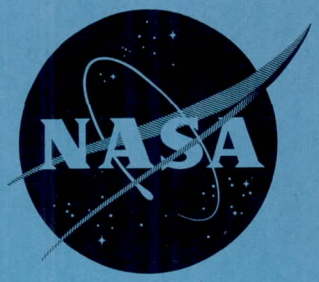

TECHNICAL MEMORANDUM

X-652

EXPERIMENTAL INVESTIGATION OF A DISK-SHAPED REENTRY CONFIGURATION AT TRANSONIC AND LOW SUPERSONIC SPEEDS

By Frank A. Lazzeroni

Ames Research Center
Moffett Field, Calif.

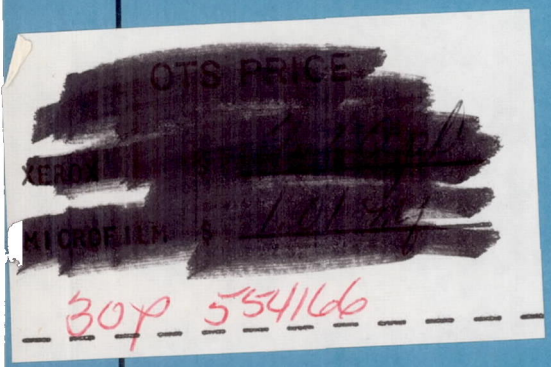

NATIONAL AERONAUTICS AND SPACE ADMINISTRATION

WASHINGTON

May 1962

copy 1

Code 1

CASE FILE COPY

NATIONAL AERONAUTICS AND SPACE ADMINISTRATION

TECHNICAL MEMORANDUM X-652

EXPERIMENTAL INVESTIGATION OF A DISK-SHAPED REENTRY CONFIGURATION AT TRANSONIC AND LOW SUPERSONIC SPEEDS*

By Frank A. Lazzeroni

SUMMARY

An investigation has been made to determine the static longitudinal and lateral-directional aerodynamic characteristics of a disk-shaped reentry configuration. The model had an elliptic profile with a maximum thickness-diameter ratio of 0.325. The tests were conducted to maximum angles of attack and sideslip of 22° over a Mach number range from 0.95 to 1.50 at a Reynolds number of 3.5×10^{6}.

The basic disk was longitudinally unstable about a center of gravity at 40 percent of the diameter from the leading edge. Addition of a canopy, vertical stabilizing surfaces, and horizontal control surfaces provided static longitudinal and directional stability through the angle-of-attack range at Mach numbers above 1.0. At a Mach number of 0.95, a slight pitch-up occurred at angles of attack above 5°.

INTRODUCTION

The design of a space vehicle capable of reentering the earth's atmosphere at satellite speed and above involves many compromises to cope with the problems of aerodynamic heating, stability and control, vehicle performance, etc. As a result, both lifting and nonlifting vehicles have been considered and the resulting shapes have been extremely varied (e.g., refs. 1 through 4). For manned flight, the lifting-type vehicle is especially attractive. One such vehicle receiving consideration is the lenticular shape. This vehicle would enter the atmosphere at a high angle of attack (50° to 90°) to produce a high drag and reduce heating; then, as the velocity decreased and the high heating period

*Title Unclassified

passed, the angle of attack would be reduced and the vehicle would enter a gliding phase. It is intended that the vehicle would be landed by conventional techniques.

It was recognized that control in low-speed flight could be a problem for the unorthodox disk-shaped vehicle. Accordingly, a study was conducted in the Ames 12-Foot Pressure Wind Tunnel of this phase of the flight regime of such vehicles (refs. 5 and 6). Out of this study two particular shapes appeared sufficiently promising to warrant some study at supersonic speed and were the subject of an investigation at a Mach number of 2.2 (ref. 7). These shapes were circular in plan form with elliptic cross sections and incorporated control and stabilizing surfaces at the rear of the vehicle and a canopy. One model had a thickness-to-diameter ratio of 0.325 and a symmetrical section and was the subject of an investigation at a Mach number of 3.5 (ref. 8). The present report presents the results of an investigation with a model having this same geometry at Mach numbers from 0.95 to 1.50 and a Reynolds number of 3.5×10^6 based on the plan-form diameter. Previous test results for uncambered circular disks have shown stable trim points at high angles of attack at transonic and supersonic speeds (refs. 8, 9, and 10). Lower angles of attack are more appropriate to this speed regime for such vehicles so the present study was confined to angles of attack less than 24°.

A 6 1 4

NOTATION

The results are presented in standard coefficient form. Lift and drag coefficients are referred to the wind axes; all other aerodynamic coefficients are referred to the body axes. All moments are referred to a point in the longitudinal plane of symmetry on the major axis of the elliptical cross section 0.40 diameter aft of the leading edge. The reference area in each case is the plan-form area of the particular configuration (including the area of the horizontal control surfaces for the complete model).

C_D drag coefficient, $\frac{\text{drag}}{qS}$

C_{D_o} drag at zero lift

C_L lift coefficient, $\frac{\text{lift}}{qS}$

C_Y side-force coefficient, $\frac{\text{side force}}{qS}$

C_l rolling-moment coefficient, $\frac{\text{rolling moment}}{qSd}$

C_m pitching-moment coefficient, $\frac{\text{pitching moment}}{qSd}$

C_n yawing-moment coefficient, $\frac{\text{yawing moment}}{qSd}$

d diameter

$\frac{L}{D}$ lift-drag ratio

M free-stream Mach number

q free-stream dynamic pressure

R Reynolds number, $\frac{\rho V d}{\mu}$

r radial distance from center of model

S plan-form area of model (including horizontal control surface area for the complete model)

$\frac{t}{d}$ maximum thickness-to-diameter ratio

V free-stream velocity

y vertical distance from chord plane

α angle of attack, measured with respect to the chord plane

β angle of sideslip

δ deflection of horizontal control surface, positive downward (see fig. 1)

ρ free-stream density

μ free-stream viscosity

$\left(\frac{dC_L}{d\alpha}\right)_{\alpha=0^\circ \text{ to } 5^\circ}$ lift curve slope between $\alpha = 0^\circ$ and 5°, per deg

$\left(\frac{dC_m}{dC_L}\right)_{C_L=0 \text{ to } 0.1}$ pitching-moment curve slope from $C_L = 0$ to 0.1

C_{Y_β}
C_{l_β}
C_{n_β} $\Big\}_{\beta=0^\circ \text{ to } 5^\circ}$ derivatives with respect to β, between $\beta = 0^\circ$ and 5°, per deg

APPARATUS AND MODEL

The experimental investigation was conducted in the Ames 6- by 6-Foot Supersonic Wind Tunnel which is of the closed-circuit variable-pressure type with a Mach number range from 0.7 to 2.2. A dimensional drawing of the model is presented in figure 1, and a photograph of the model is shown in figure 2. The basic shape was circular in plan form with a thickness-to-diameter ratio of 0.325 and an elliptic profile, the shape being generated by revolving, about the minor axis, the elliptic sections defined by the coordinates given in table I.

The horizontal control surfaces were thick flat plates extending radially from the trailing edge of the basic disks as shown in figure 1. The horizontal control surfaces consisted of two inboard and two outboard surfaces with a total area which was 25 percent of the plan-form area of the basic disk. The hinge lines of the controls were normal to radial lines of the disk at the centers of the respective controls.

The vertical stabilizing surfaces were two constant thickness triangular shapes with rounded leading edges swept back 65°. Each vertical surface was 5-1/2 percent of the plan-form area of the basic disk, giving a total exposed area of 11 percent of the plan-form area.

Details of the model canopy are shown in figure 3. A small fairing at the rear of the models accommodated the support sting. An internal six-component strain-gage balance was used to measure the forces and moments on the model.

TEST AND PROCEDURES

Measurements of the static longitudinal aerodynamic characteristics of the model were made at Mach numbers from 0.95 to 1.50 for a Reynolds number of 3.5 million based on the diameter of the model. The angle-of-attack and angle-of-sideslip ranges were from -6° to +22° and the horizontal control surface deflections were from -20° to +5°.

Stream Variations

Surveys of the stream characteristics of the wind tunnel have shown that essentially no stream curvature exists in the vicinity of the model and that the axial static-pressure variations are less than 1 percent of the dynamic pressure. Therefore, no corrections for stream curvature or static-pressure variations were made in the present investigation. The data have been adjusted to take account of the stream angles in the vertical plane along the tunnel center line measured in these surveys.

Support Interference

Interference from the sting support on the aerodynamic characteristics of the model was considered to consist primarily of a change in the pressure at the base of the model. Accordingly, the static pressures within the balance cavity of the model were measured and the drag data were adjusted to correspond to free-stream static pressure within the cavity and on the base of the annulus of the model fairing around the sting.

Tunnel-Wall Interference

The effectiveness of the perforations in the wind-tunnel test section in preventing choking and in absorbing reflected disturbances at low supersonic speeds has been established experimentally. Unpublished data from the wind-tunnel calibration indicate that reliable data can be obtained throughout the Mach number range of the tunnel if certain restrictions are imposed on the model size and attitude. The configuration used in the present investigation complied with these restrictions and shadowgraph observations of the flow around the model substantiated the fact that no choking or reflected disturbances were present for the test conditions reported herein.

RESULTS

The results of the experimental investigation are presented in figures 4 through 9. Longitudinal aerodynamic characteristics of the basic disk are presented in figure 4. Lift and pitching-moment curve slopes and drag at zero lift are shown as functions of Mach number in figure 5 for the basic disk. Data from $M = 0.25$ to $M = 0.9$ were obtained from reference 6 while data at $M = 2.2$ were obtained from reference 7. Longitudinal and lateral-directional aerodynamic characteristics of the complete model with canopy, vertical surface, and horizontal control

surfaces are presented in figures 6 and 7, respectively, while the lift and pitching-moment curve slopes and drag at zero lift as a function of Mach number are summarized in figure 8. The lateral-directional stability derivatives are summarized in figure 9. As with the basic disk, the summary data from $M = 0.25$ to 0.90 and at $M = 2.2$ for figures 8 and 9 were obtained from references 6 and 7, respectively.

With the center of moments 0.4 diameter aft of the leading edge, the slope of the pitching-moment curve for the basic disk (figs. 4 and 5) had a positive value at low lift coefficients and decreased to zero or became slightly negative at higher lift coefficients. When the canopy, vertical surfaces, and horizontal control surfaces at zero deflection were added to the basic disk, the pitching-moment curves had a stable slope throughout the Mach number range of the present investigation (figs. 6 and 8). Upward (negative) deflection of the horizontal controls reduced the static longitudinal stability at Mach numbers of 0.95, 1.00, and 1.10 (figs. 6(a), (b), and (c)), and neutral or slightly unstable conditions were present for certain lift coefficients, depending on the Mach number. At Mach numbers of 1.30 and 1.50 (figs. 6(d) and (e)) the pitching-moment curves with the controls deflected were more linear than at the lower Mach numbers, and stable trim conditions were evident to near maximum L/D. The effects of control deflection on L/D were small for the Mach number range of the investigation.

A 6 1 4

The yawing-moment and side-force data presented in figure 7 indicate that the vertical surfaces maintain their effectiveness to high angles of sideslip throughout the transonic speed range at angles of attack of 0° and 5°. The rolling-moment data indicate that the vertical surfaces provide a negative increment of dihedral effect at low angles of attack in the transonic speed range. The summary of results in figure 9 for the complete model shows a reduction of directional stability with increasing Mach number in the supersonic speed range and a negative dihedral effect at transonic speeds for an angle of attack of 0°. The dihedral effect was positive throughout the speed range for an angle of attack of 5°.

Ames Research Center
National Aeronautics and Space Administration
Moffett Field, Calif., Mar. 6, 1962

REFERENCES

1. Staff of Langley Flight Research Division (compiled by Donald C. Cheatham): A Concept of a Manned Satellite Reentry Which is Completed With a Glide Landing. NASA TM X-226, 1959.

2. Foster, Gerald V.: Exploratory Investigation at a Mach Number of 2.01 of the Longitudinal Stability and Control Characteristics of a Winged Reentry Configuration. NASA TM X-178, 1959.

3. Eggers, Alfred J., Jr., and Wong, Thomas J.: Re-entry and Recovery of Near-Earth Satellites, With Particular Attention to a Manned Vehicle. NASA MEMO 10-2-58A, 1958.

4. Grant, C. Frederick: Importance of the Variation of Drag With Lift in Minimization of Satellite Entry Acceleration. NASA TN D-120, 1959.

5. Demele, Fred A., and Brownson, Jack J.: Subsonic Longitudinal Aerodynamic Characteristics of Disks With Elliptic Cross Sections and Thickness-Diameter Ratios From 0.225 to 0.425. NASA TN D-788, 1961.

6. Demele, Fred A., and Brownson, Jack J.: Subsonic Aerodynamic Characteristics of Disk Re-entry Configurations With Elliptic Cross Sections and Thickness-Diameter Ratios of 0.225 and 0.325. NASA TM X-566, 1961.

7. Lazzeroni, Frank A.: Aerodynamic Characteristics of Two Disk Re-entry Configurations at a Mach Number of 2.2. NASA TM X-567, 1961.

8. Demele, Fred A., and Lazzeroni, Frank A.: Effects of Control Surfaces on the Aerodynamic Characteristics of a Disk Re-entry Shape at Large Angles of Attack and a Mach Number of 3.5. NASA TM X-576, 1961.

9. Mugler, John P., Jr., and Olstad, Walter B.: Static Longitudinal Aerodynamic Characteristics at Transonic Speeds of a Lenticular-Shaped Reentry Vehicle, NASA TM X-423, 1960.

10. Jackson, Charlie M., Jr., and Harris, Roy V., Jr.: Static Longitudinal Stability and Control Characteristics at a Mach Number of 1.99 of a Lenticular-Shaped Reentry Vehicle. NASA TN D-514, 1960.

TABLE I.- COORDINATES OF SURFACE OF MODEL
[All dimensions in inches]

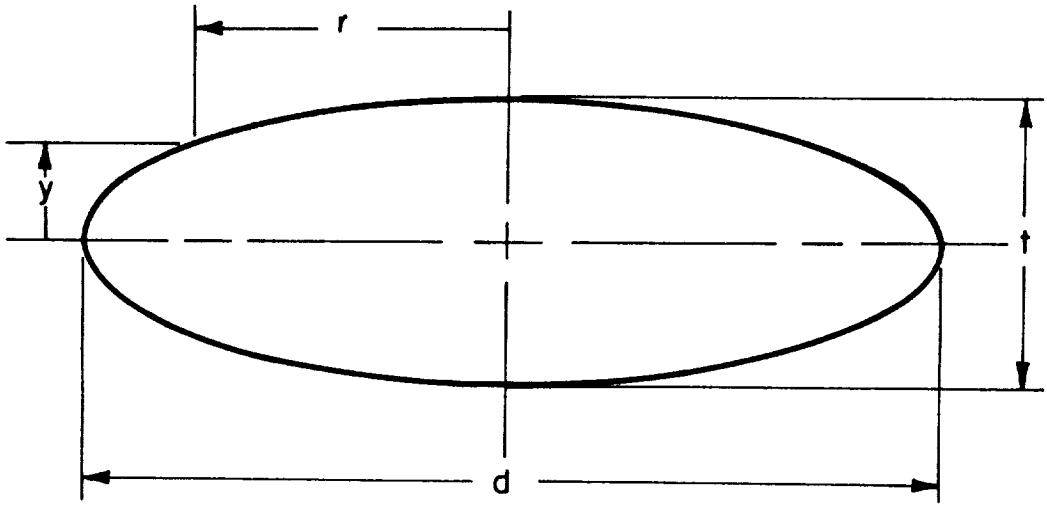

t/d = 0.325			
r	±y	r	±y
0	1.950	3.60	1.560
.25	1.948	3.75	1.522
.50	1.943	4.00	1.453
.75	1.935	4.25	1.376
1.00	1.923	4.50	1.290
1.25	1.908	4.75	1.191
1.50	1.888	5.00	1.078
1.75	1.865	5.25	.944
2.00	1.838	5.50	.779
2.25	1.808	5.60	.700
2.50	1.773	5.70	.609
2.75	1.733	5.80	.499
3.00	1.689	5.90	.355
3.25	1.639	5.95	.251
3.50	1.584	6.00	0

A 6 1 4

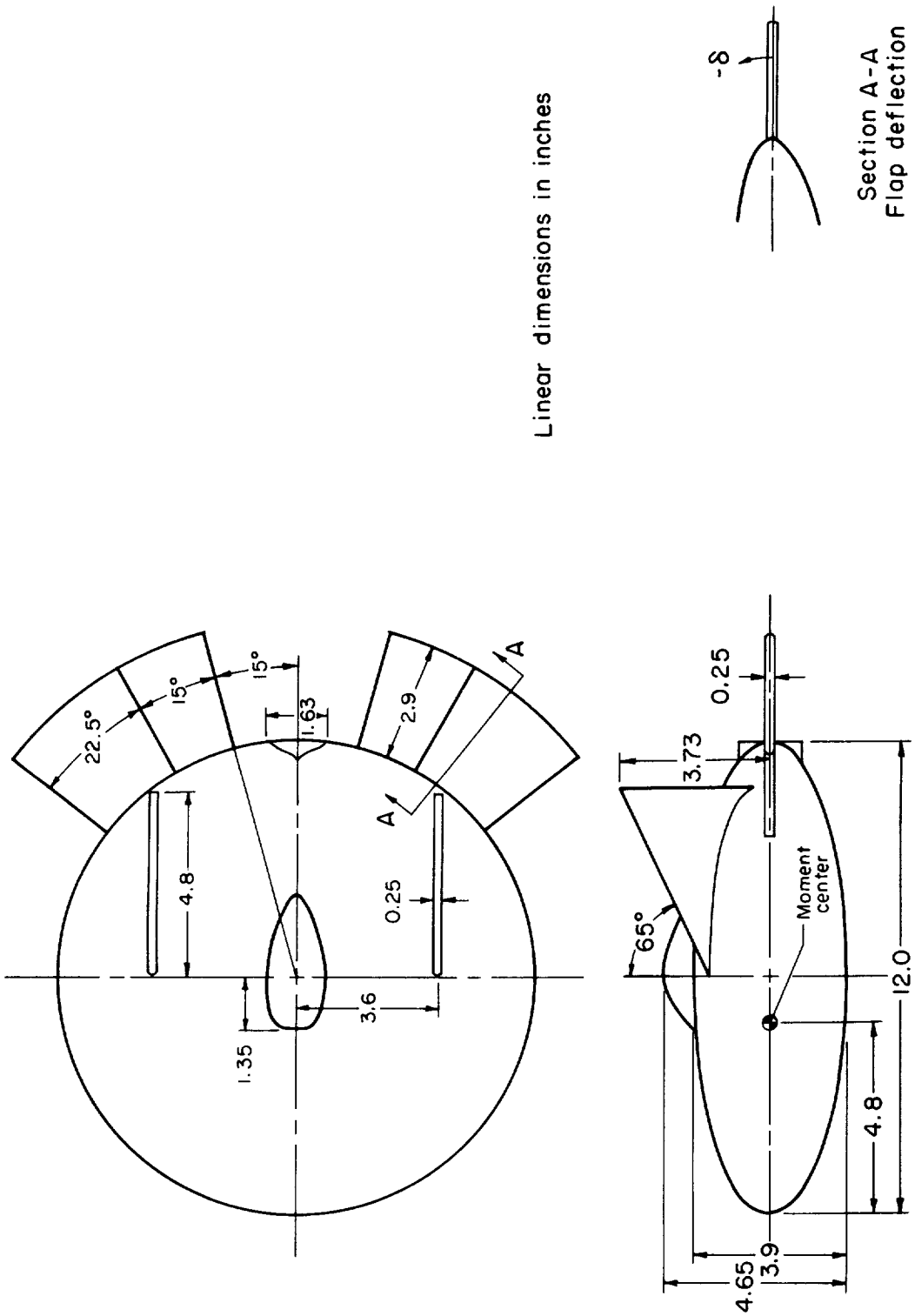

Figure 1.- Dimensional drawing of model.

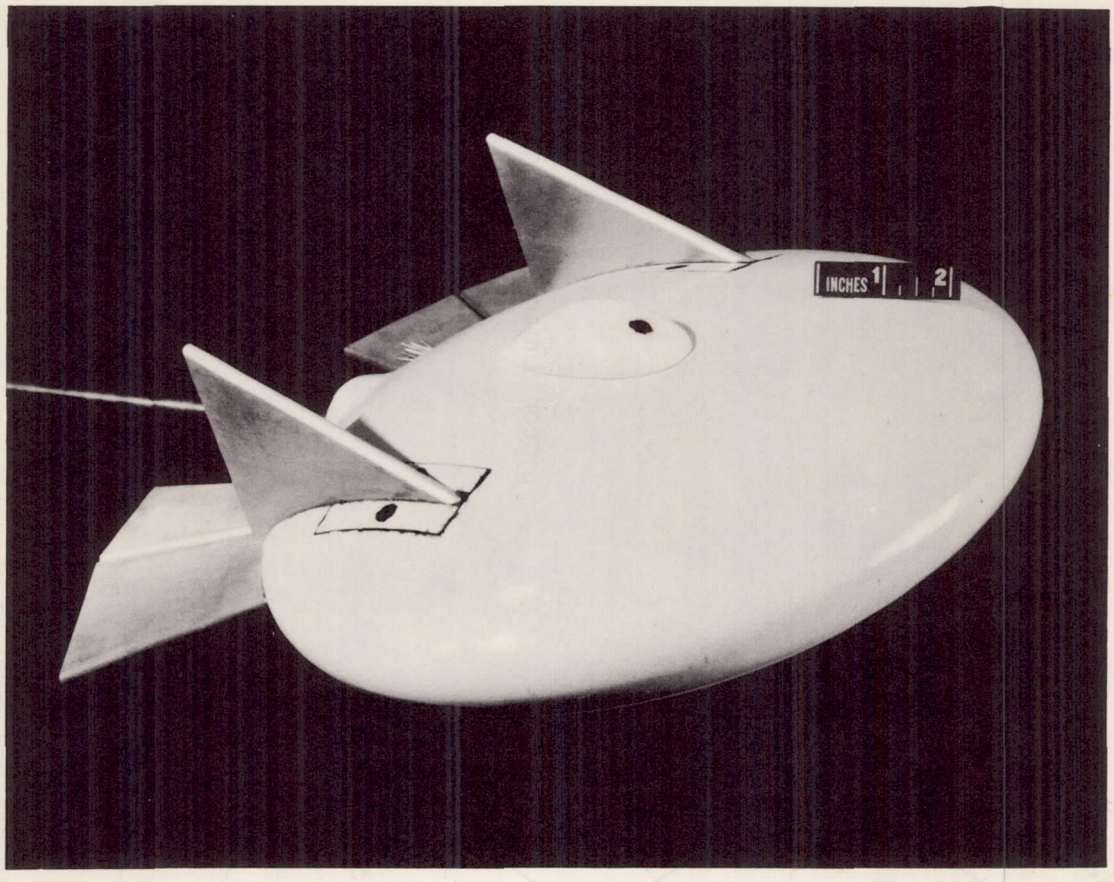

A-28583

Figure 2.- Photograph of model.

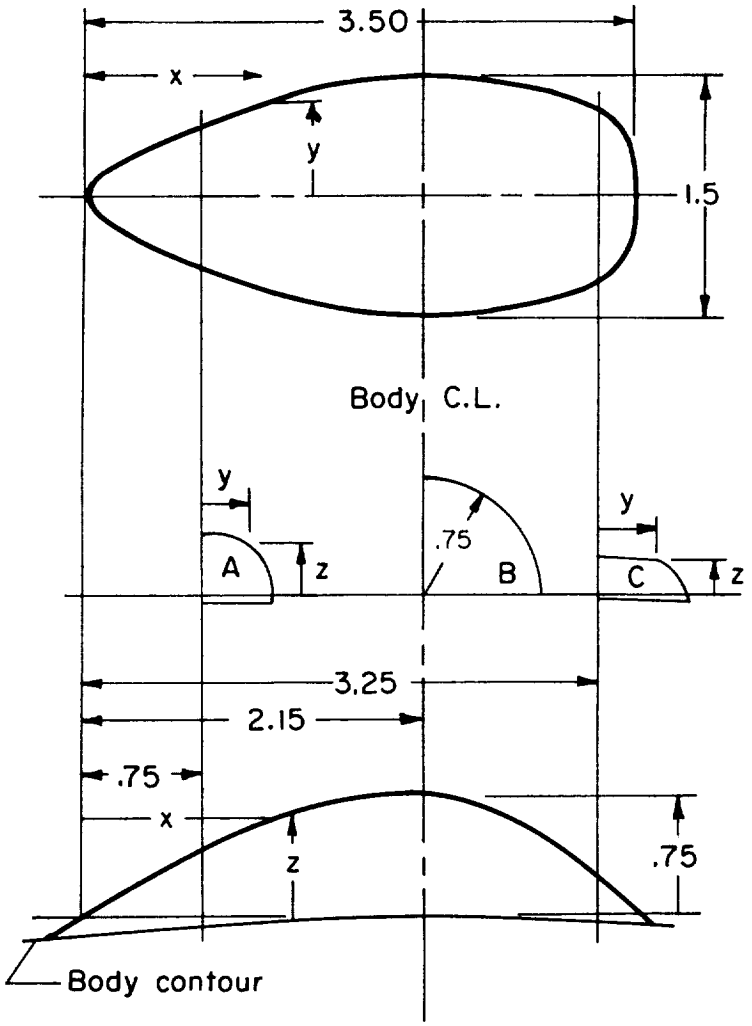

Plan		Profile		Section A		Section C	
x	y	x	z	y	z	y	z
0	0	0	0	0	0.405	0	0.245
.05	±.145	.50	.290	.10	.400	.10	.245
.25	.220	1.00	.520	.15	.395	.20	.240
.50	.345	1.50	.680	.20	.380	.25	.235
1.00	.545	2.15	.750	.25	.365	.30	.230
1.50	.690	2.50	.680	.30	.340	.35	.220
2.15	.750	3.00	.425	.35	.295	.40	.205
2.50	.735	3.50	0	.40	.235	.45	.180
3.00	.655			.45	0	.50	.130
3.25	.550					.55	0
3.40	.410						
3.50	0						

Figure 3.- Canopy details.

(a) C_L vs. α, C_L vs. C_D

Figure 4.- Static longitudinal aerodynamic characteristics of the basic disk.

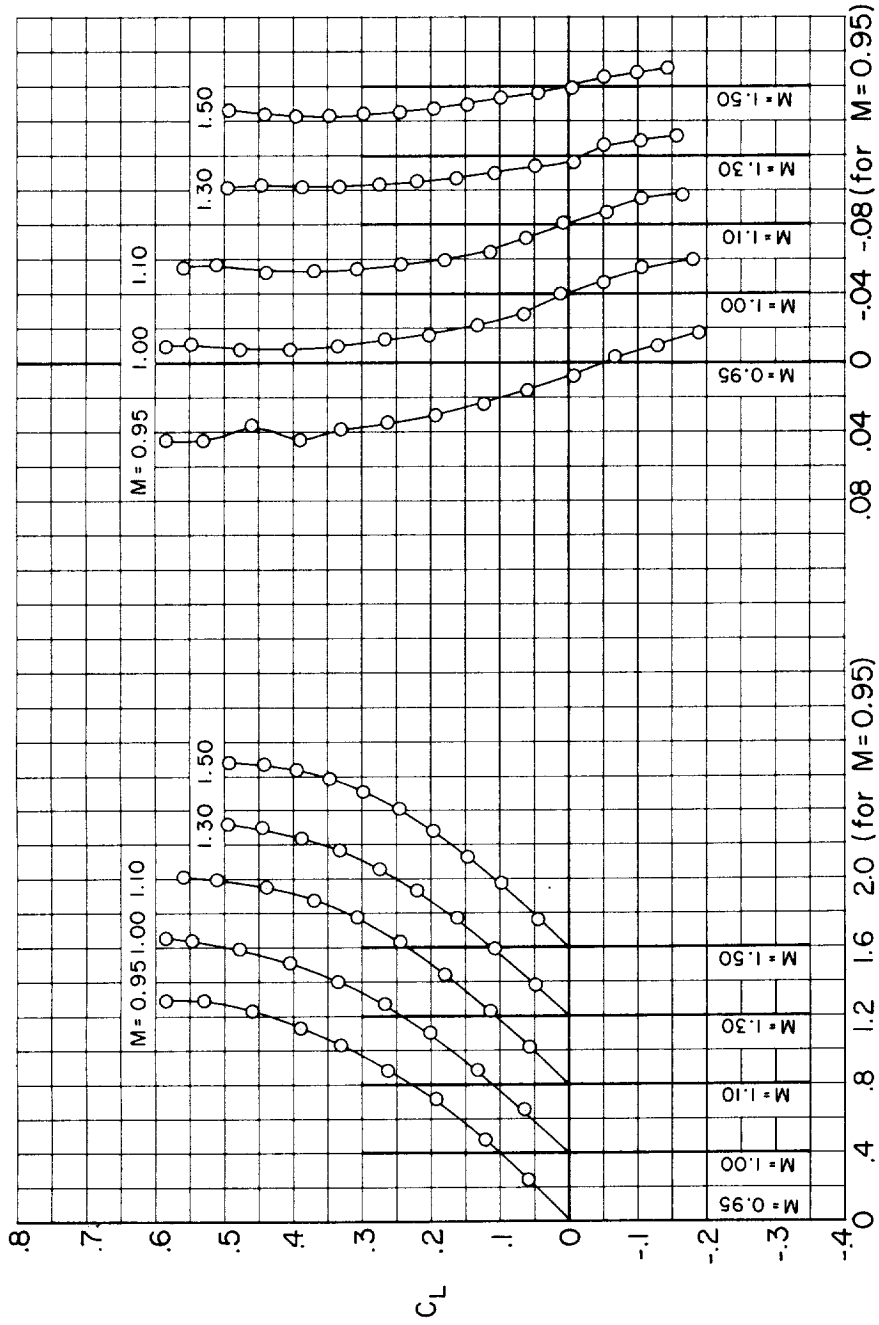

(b) C_L vs. L/D, C_L vs. C_m

Figure 4.- Concluded.

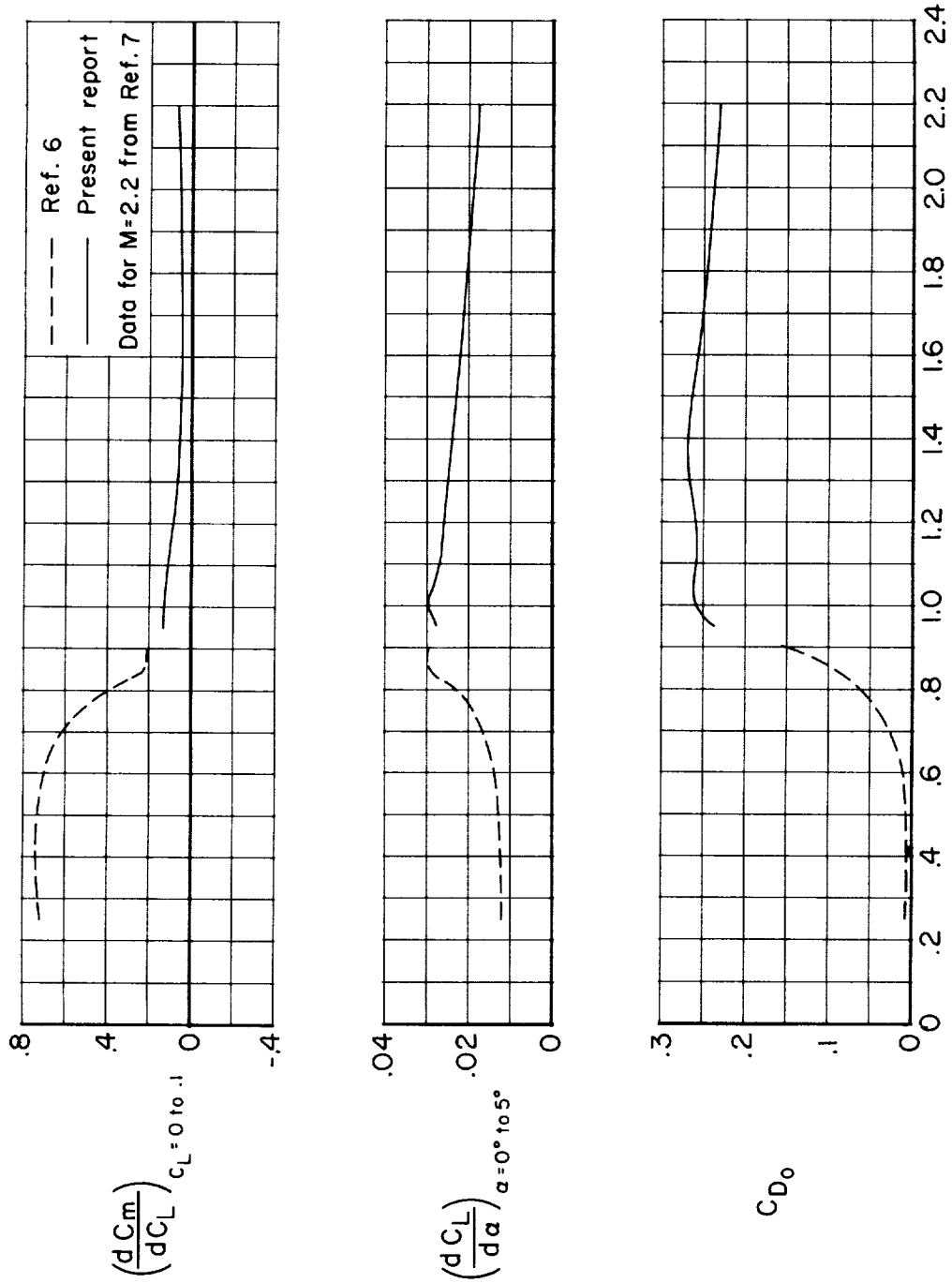

Figure 5.- The variation with Mach number of lift curve slope, pitching-moment curve slope, and drag at zero lift for the basic disk.

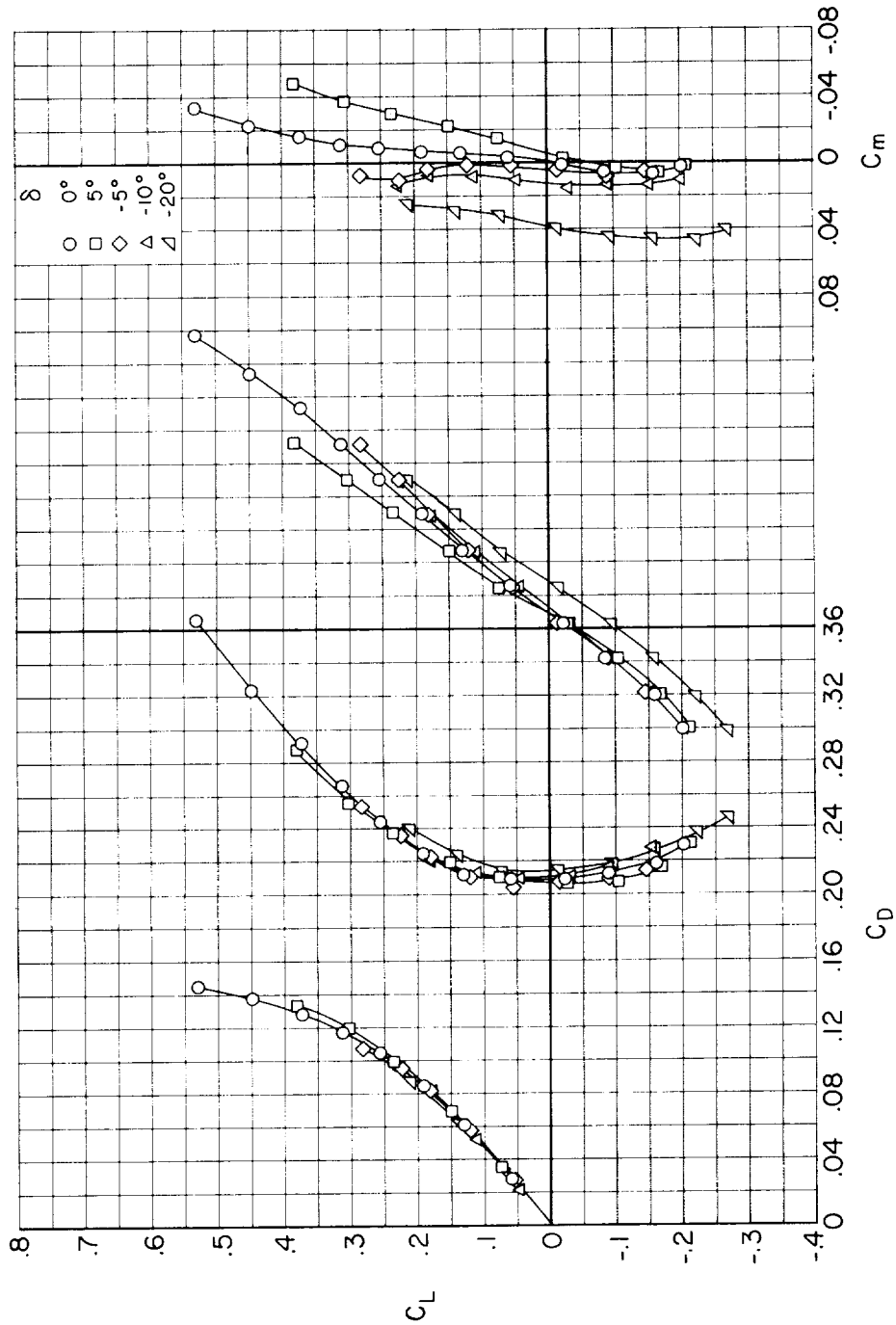

(a) M = 0.95

Figure 6.- Effect of horizontal control surface deflection on the aerodynamic characteristics of the complete model.

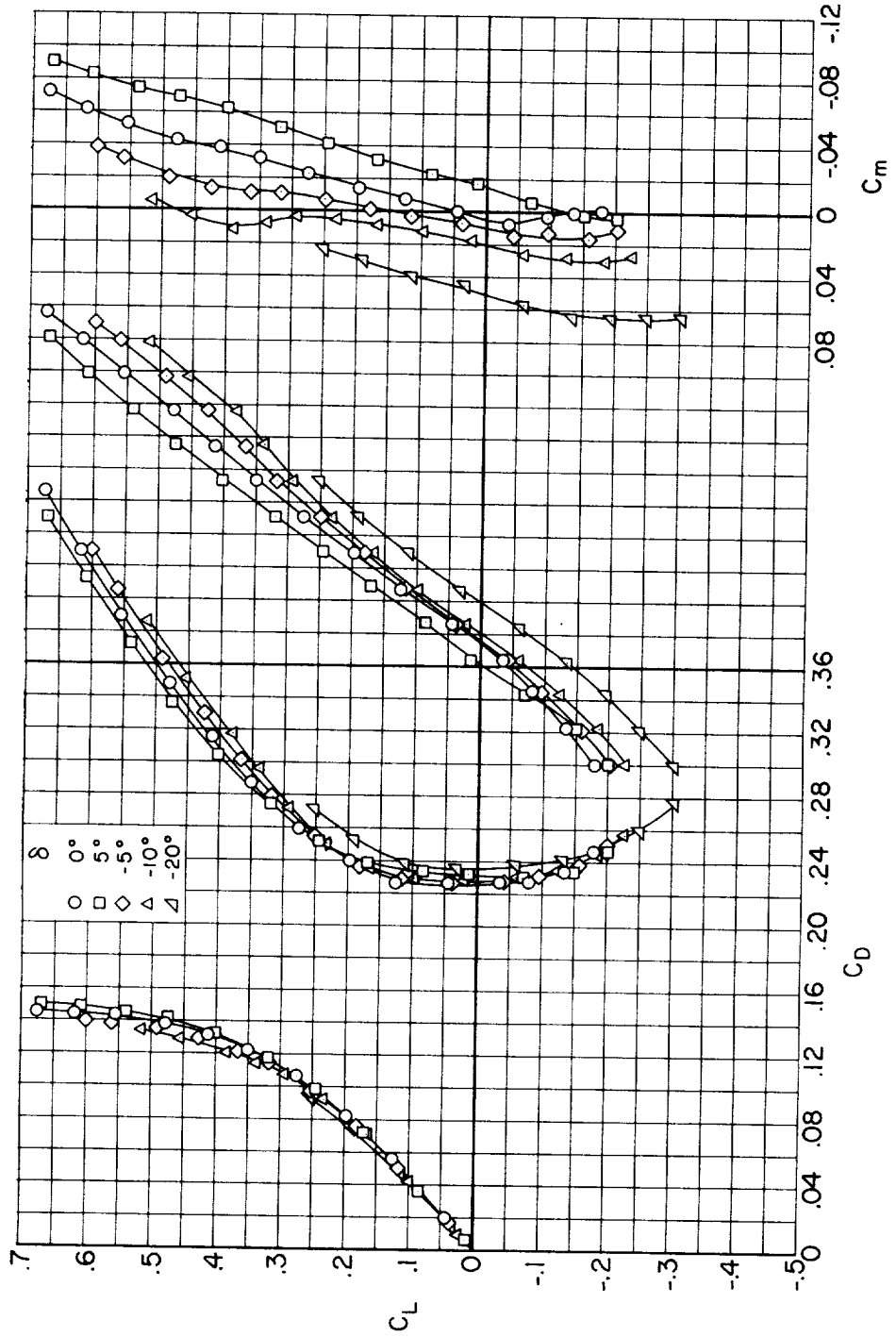

(b) M = 1.00

Figure 6.- Continued.

A 6 1 4

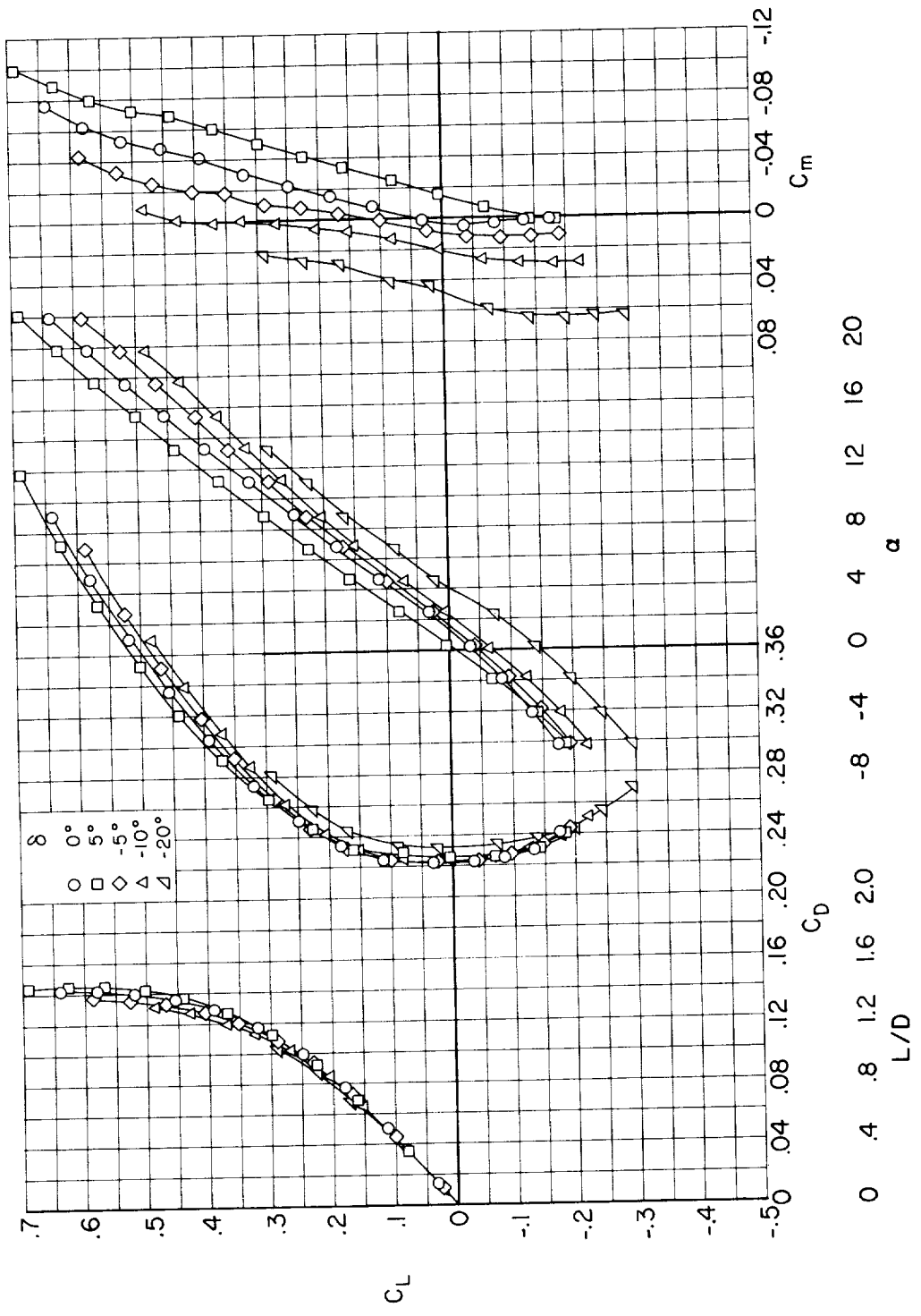

(c) M = 1.10

Figure 6.- Continued.

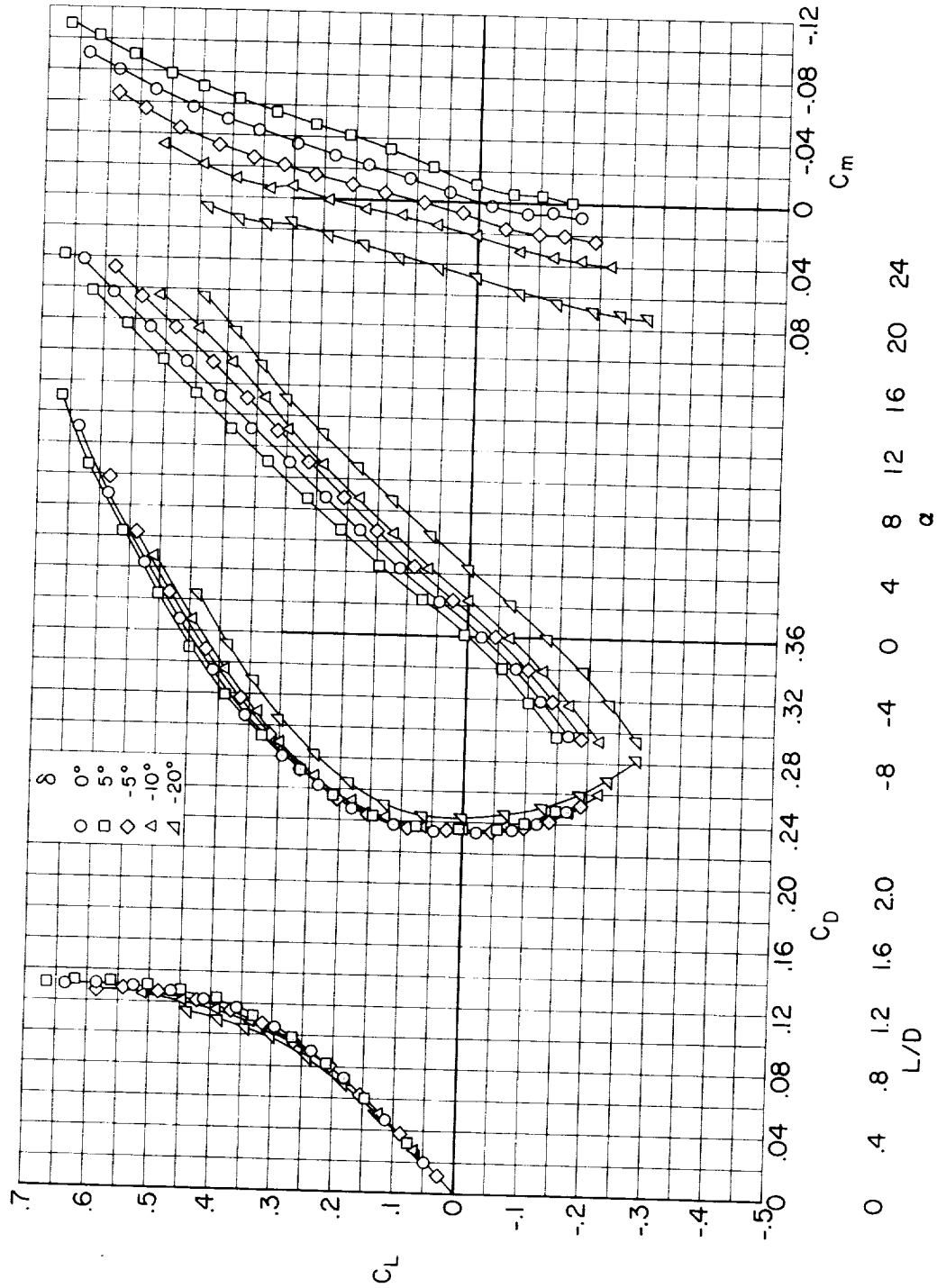

(d) M = 1.30

Figure 6.- Continued.

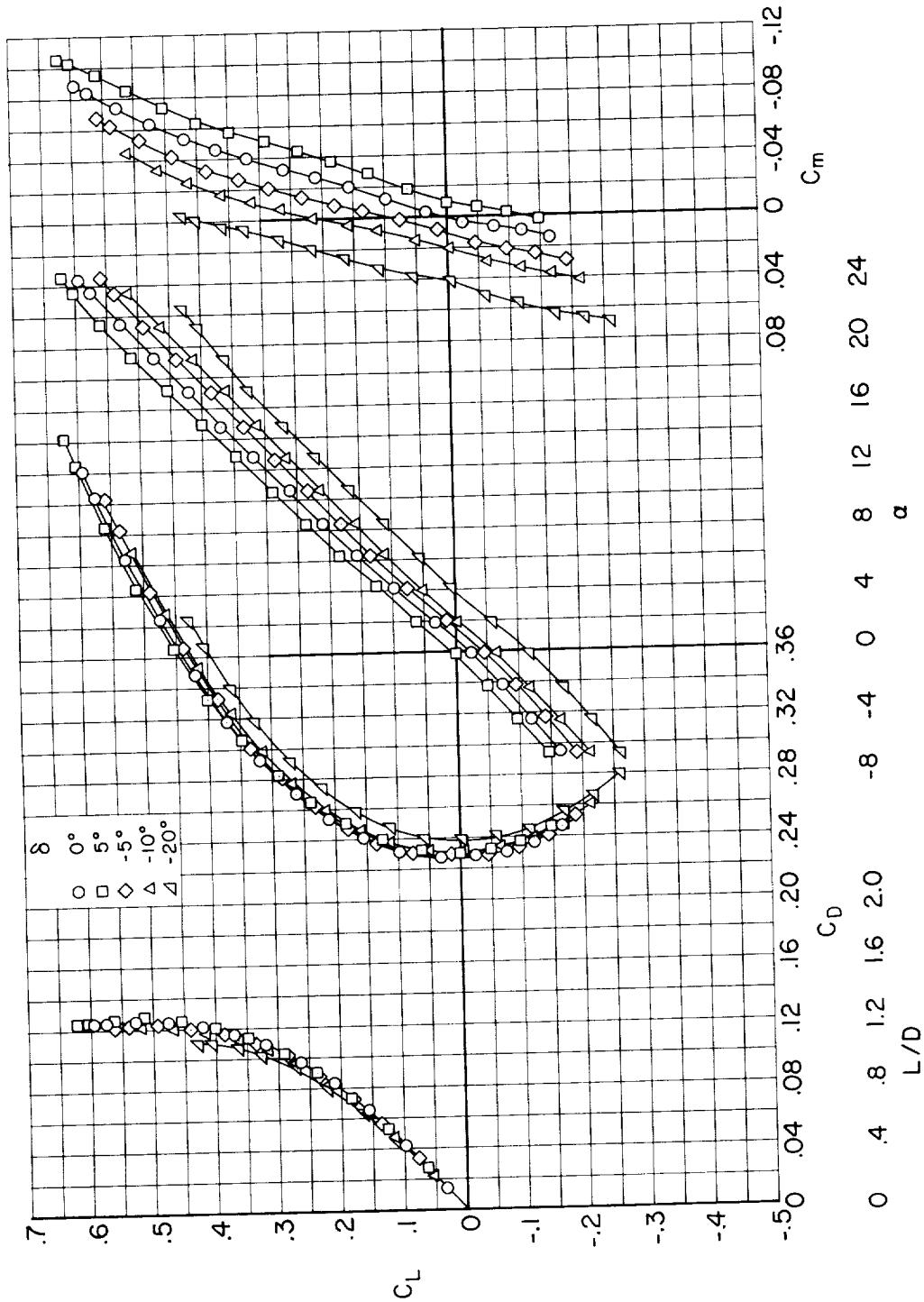

(e) M = 1.50

Figure 6.- Concluded.

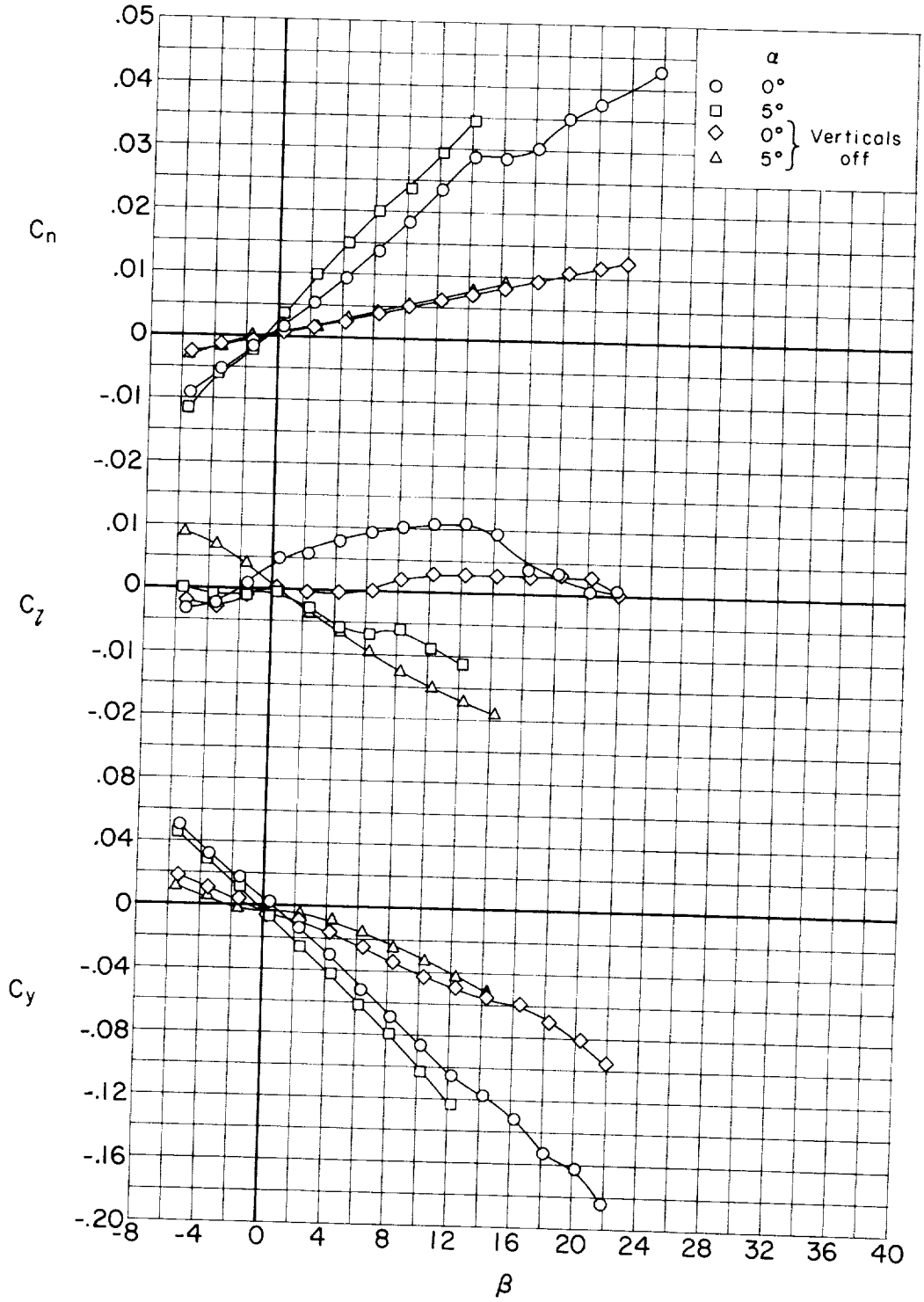

(a) M = 0.95

Figure 7.- Static lateral-directional aerodynamic characteristics of the complete model.

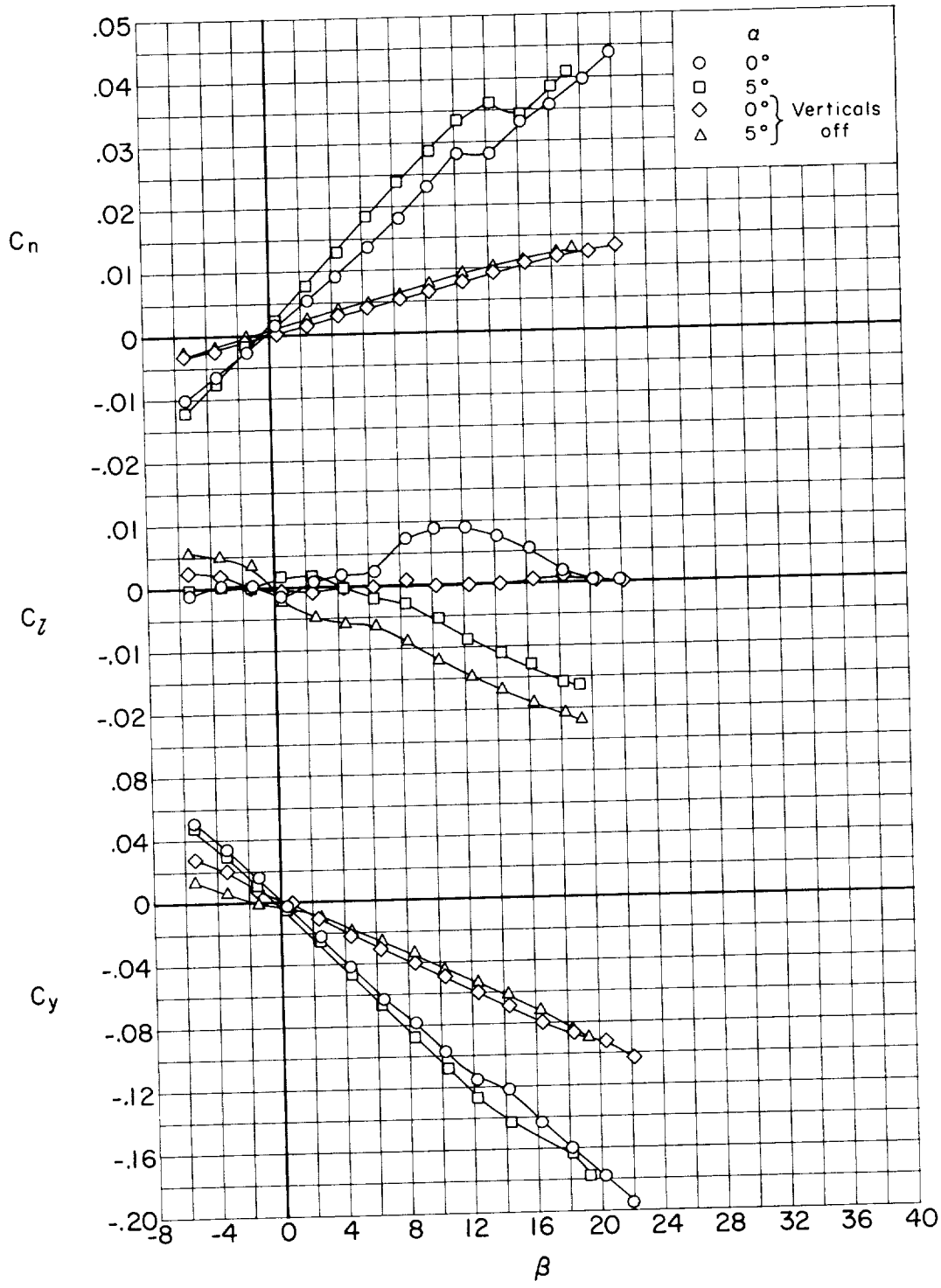

(b) M = 1.00

Figure 7.- Continued.

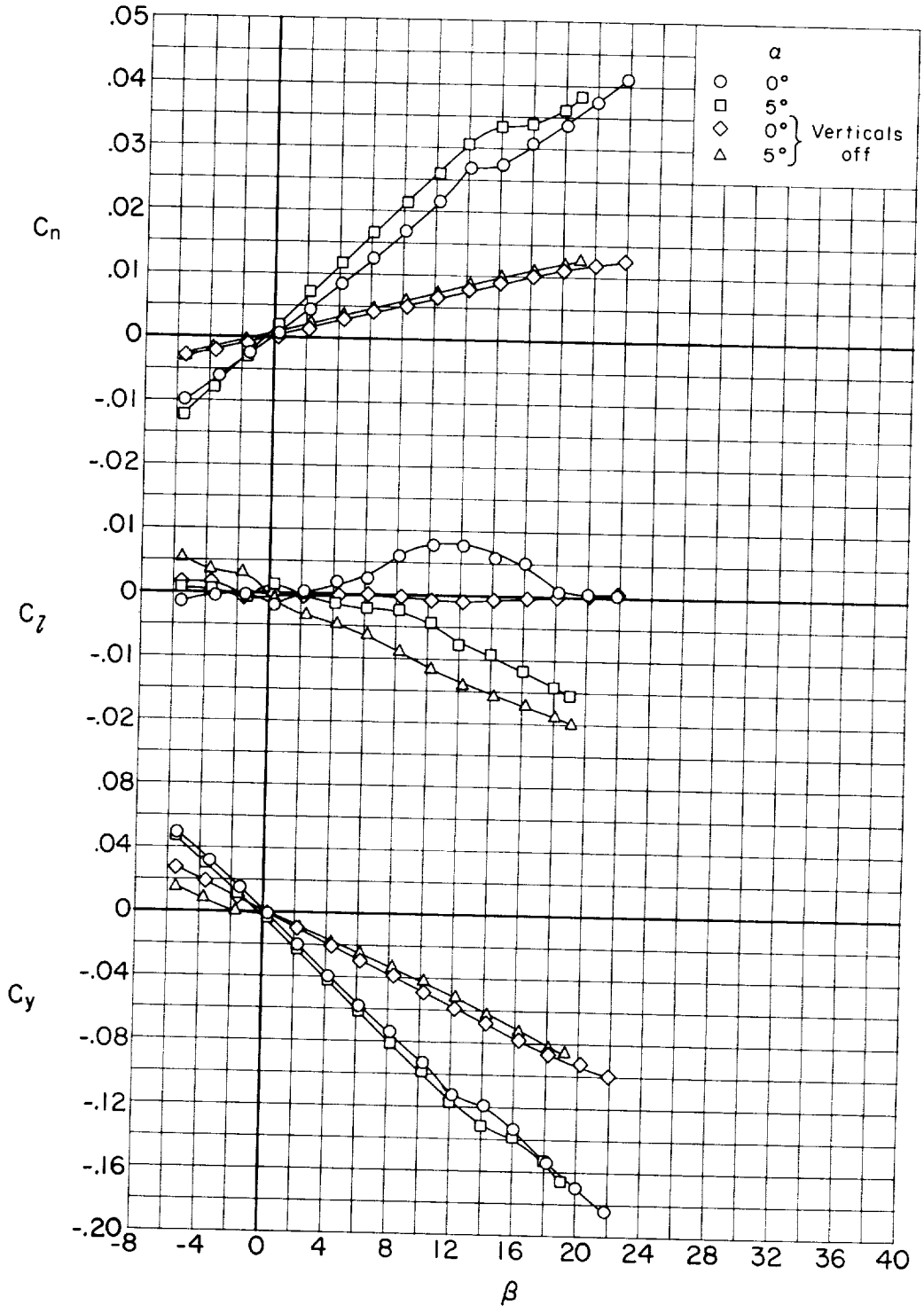

(c) M = 1.10

Figure 7.- Continued.

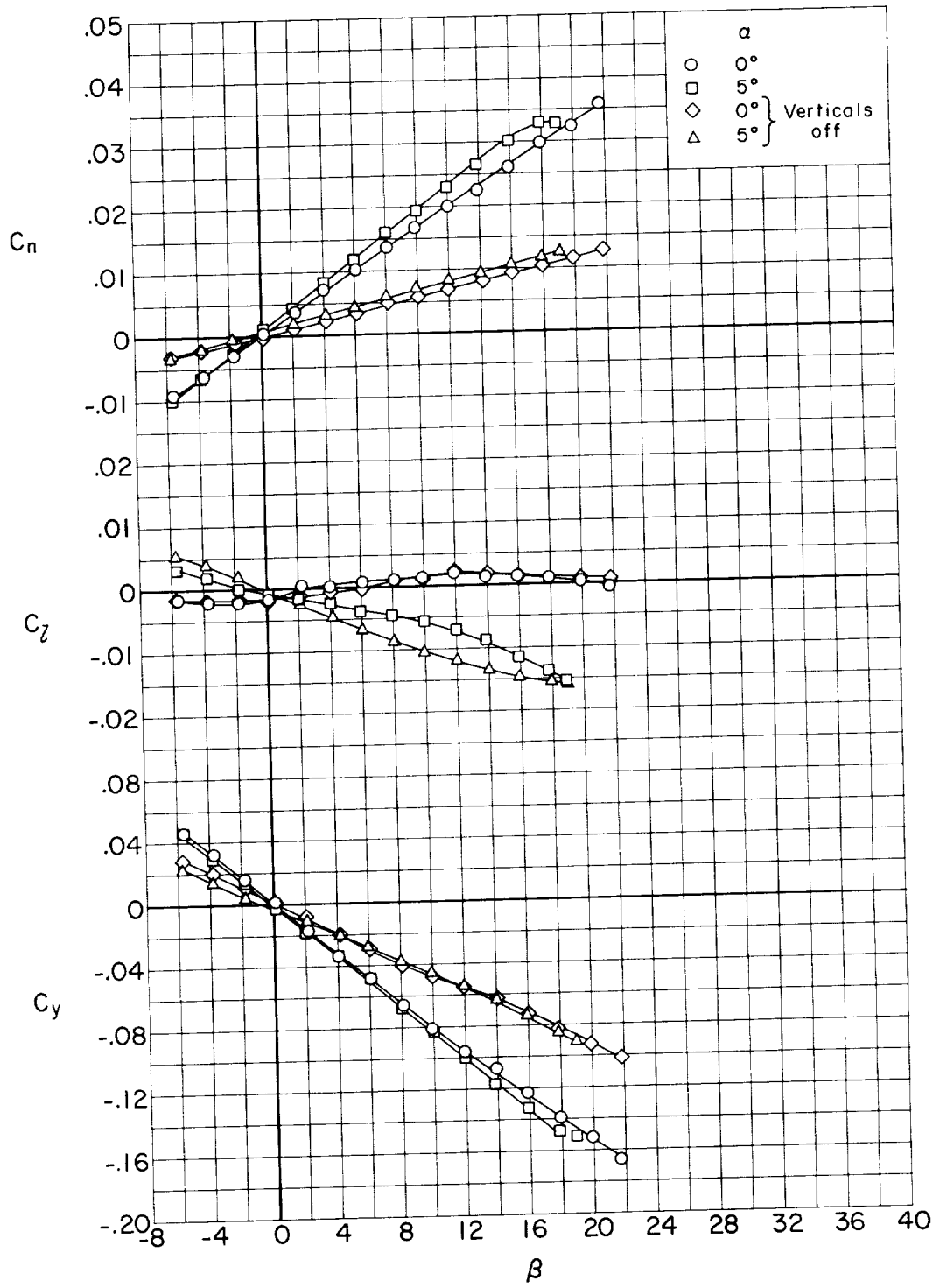

(d) M = 1.30

Figure 7.- Continued.

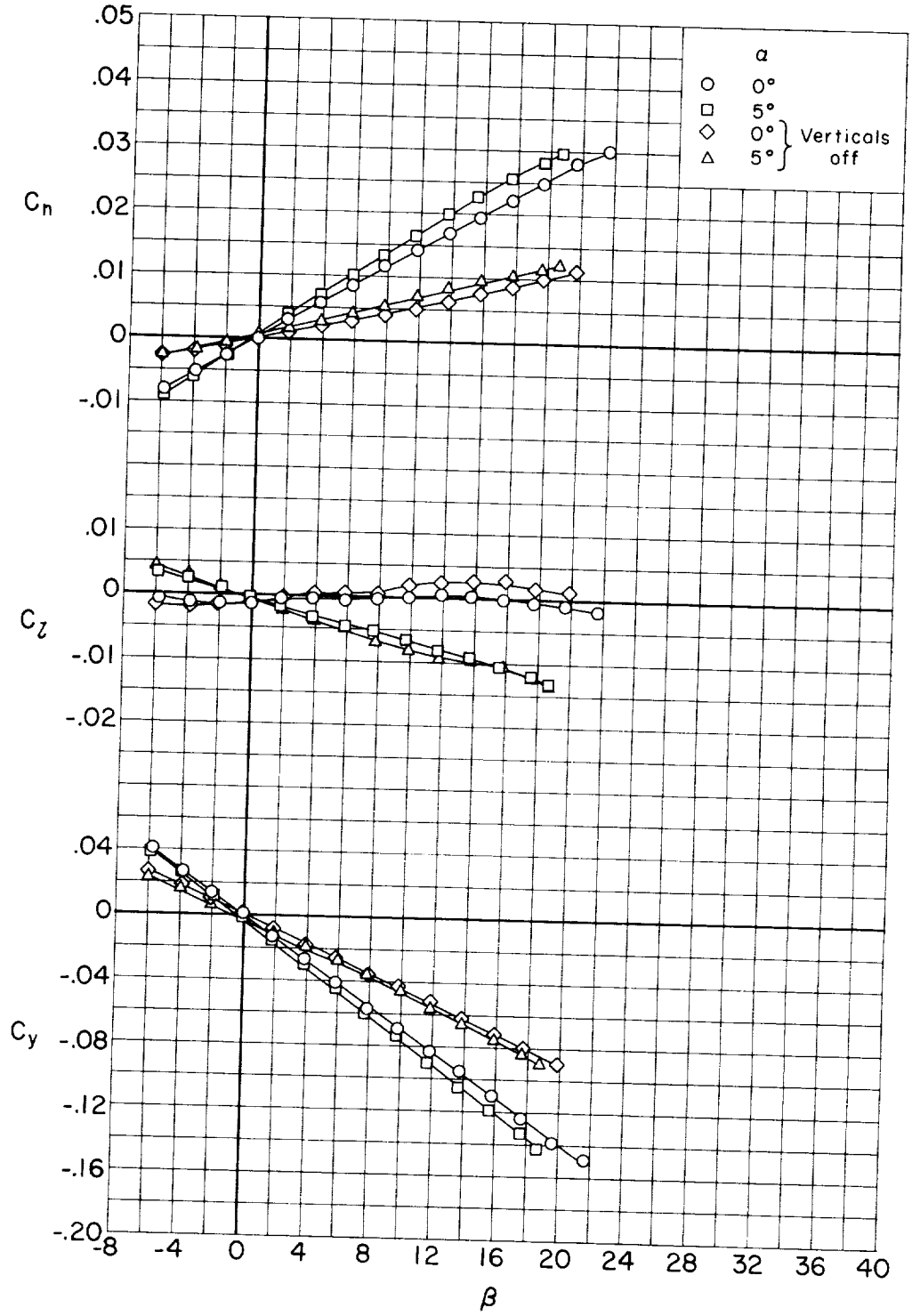

(e) M = 1.50

Figure 7.- Concluded.

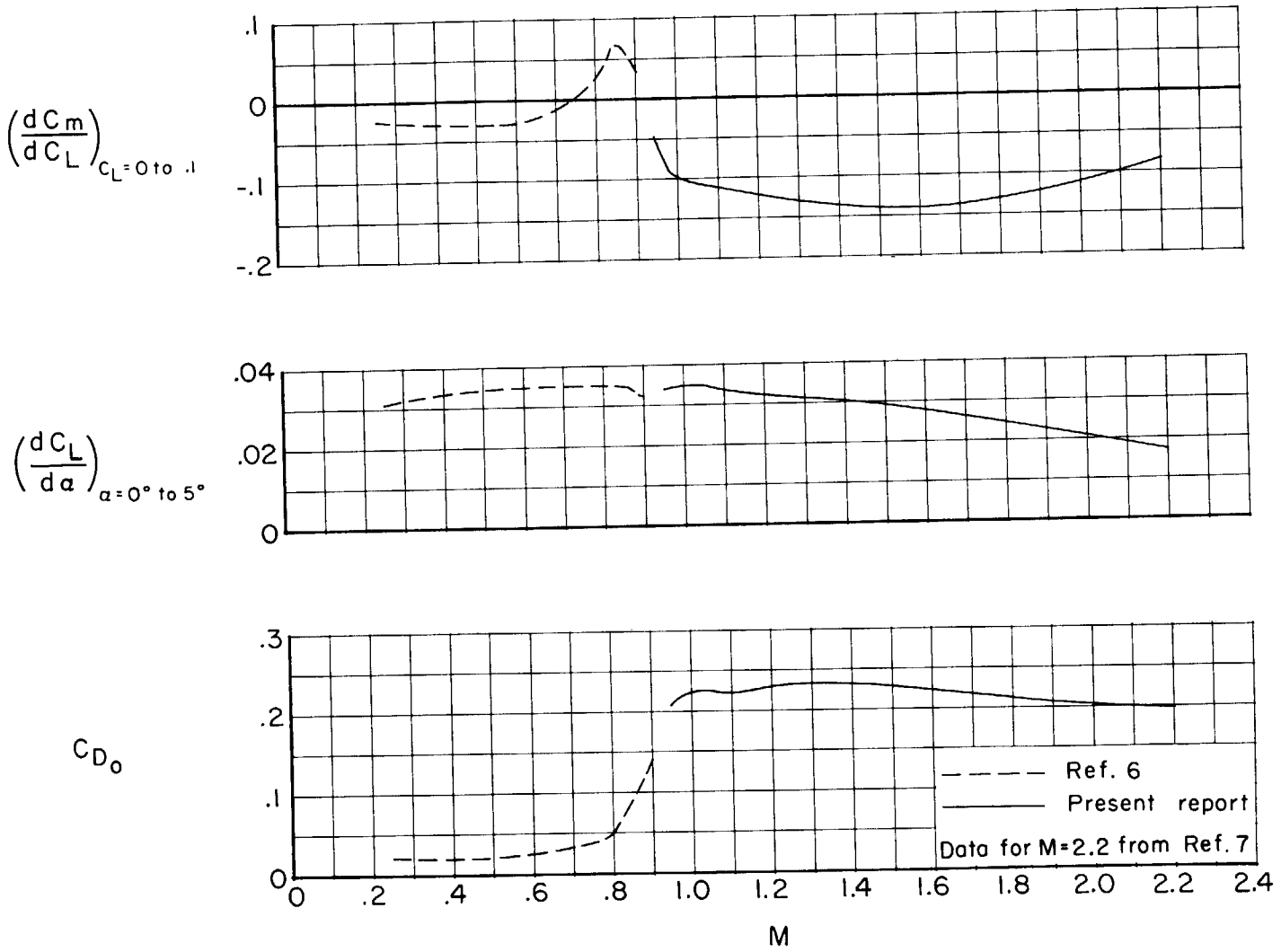

Figure 8.- The variation with Mach number of lift curve slope, pitching-moment curve slope, and drag at zero lift for the complete model.

CONFIDENTIAL

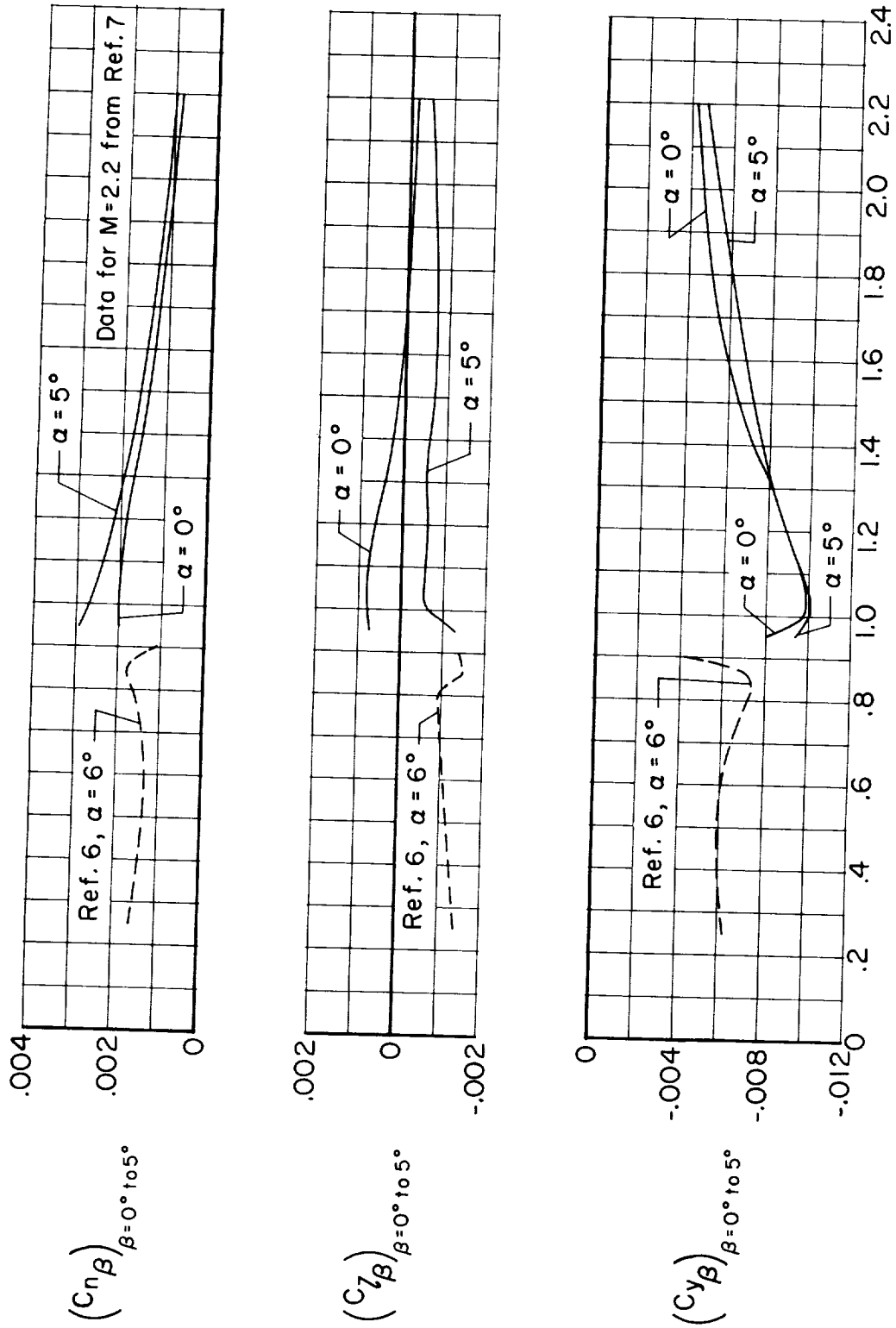

Figure 9.- The variation with Mach number of the lateral stability derivatives of the complete model.

A 6 1 4

UNCLASSIFIED